# Optically active μ-disks resonators-based sensor for refractive index variation detection.

F. Ferrarese Lupi*[a], D. Navarro-Urrios [b], J. Rubio-Garcia [c], J. Monserrat [d], C. Domínguez [d], B. Garrido[a]

[a] MIND-IN2UB, Dept. Electrònica, Universitat de Barcelona, C/Martí i Franquès 1, 08028, Barcelona, Spain; [b] Catalan Institute of Nanotechnology (CIN2-CSIC), Campus UAB, Edifici CM3, 08193 Bellaterra (Barcelona), Spain; [c] Laboratori d'Emmagatzematge d'Energia i Sistemes Autònomsnstitut de Recerca en Energia de Catalunya (IREC), Barcelona, Spain; [d] Instituto de Microelectrònica de Barcelona-Centre Nacional de Microelectrònica, Consejo Superior de Investigaciones Científicas, Bellaterra, E-08193, Barcelona, Spain.

## ABSTRACT

The design, optical characterization and sensoristic capability provided by a complementary metal-oxide-semiconductor (CMOS) compatible integrated sensor based on a μ-disk resonator cavity are reported. The working principle of the presented device consists in monitoring the changes in the effective refractive index of the supported optical modes induced by variations of the refractive index of the surrounding material. The detection system has been designed on the base of a high quality factor ($Q$=1.4x10$^4$) Si-rich Si$_3$N$_4$ (SRSN) μ-disk - emitting in the VIS under optical pumping - bottom coupled to a low loss passive stoichiometric Si$_3$N$_4$ waveguide (WG), with losses values under 1 dB/cm measured in the same spectral region. The PL emission in the VIS range provided by the SRSN enable the use of Si-based detectors, easily integrable using the current CMOS standard technology. Proof of concept measurements performed on the coupled device revealed a good sensitivity of 51.79 nm/RIU (Refractive Index Unit), in accordance with the simulated data, and a minimum detection limit of $1.1 \times 10^{-3}$ RIU.

**Keywords:** Optical sensors, cavity resonators, active sensor, micro-disk, optical losses, photoluminescence (PL), whispering gallery mode (WGM).

## 1.    INTRODUCTION

In the last decade Si photonics has gained a principal role in the realization of miniaturized, versatile and inexpensive devices, which can be used as detection systems. Such technological field is giving new opportunities that are growing in parallel to the main goal of Si photonics, that is the research of a Si-based integrated light source: indeed a large variety of Si-based integrated photonic elements have found application in the sensoristic. [1]-[2]

Many approaches of direct detection, not always based on Si materials, have already been investigated. Among them it is worth to remark the surface plasmon resonator (SPR) [3] Mach-Zehnder interferometers [4]-[5], directional couplers [6] and optical waveguide based sensors. [7] A large part of the cited devices ensure high performances in terms detection limit (DL - minimum measurable change of refractive index of the analyte) from $10^{-5}$ to $10^{-8}$ refractive index unit (RIU) but require a relatively high interaction length with the analyte, decreasing the compactness of the system.

This problem can be overcome by using others optical elements like photonics crystals [8] or passive μ-resonators cavities having circular geometry, such as μ-disks and μ-rings [9]-[10], presenting reasonably high sensitivities (S) up to $1x10^4$ nm/RIU change, in a reduced space. On the other hand, the main issue concerning the aforesaid structures is the need of a broadband light source (broadband lamp or tunable laser, normally in the near infrared region) that has to be externally coupled into a bus waveguide. Normally this condition is accomplished using grating couplers and it cannot be easily achieved in a hand-held device.

A very interesting alternative in order to solve this problem is to combine the emission properties of an active material such as SRSN, with the optical properties of a circular resonator cavity.

*fferrarese@el.ub.es; phone +34 934 039 176; fax +34 934 021 148

There is no need for a external source of light coupled with the optical circuit, since we can directly make use of the light emitted under optical excitation by the active material. In this case the external excitation becomes a non-critical parameter because it can be obtained by roughly pumping with light a large area of the device with an incident excitation spot. Furthermore circular μ-resonators cavities present reasonably high DL and $S = 10^2$ nm/RIU [9] while maintaining a good tolerance to the fabrication accuracy.

This particular solution, together with the full CMOS compatibility deriving form the Si-based material used in the fabrication of the device, also allows an extended on-chip integration suitable for high volume production and field use.

Since it is possible to merge photonics and electronics in the same chip, we foresee this new approach as a promising starting point for low cost advanced sensor systems showing high sensitivity and extremely small footprint, allowing very small quantities of analyte to be measured.

In this paper, we present the simulation and the characterization of a basic sensing photonic structure consisting on a μ-disk cavity made of a SRSN material vertically coupled to a passive low loss stoichiometric $Si_3N_4$ WG (see Figure 1).

The operational principle of these structures is based on the effective refractive index changes of the cavity supported modes when the refractive index outside the cavity is modified. The PL spectrum emitted by the active material is modulated by the Whispering Gallery Mode (WGM) spectrum, characteristic of the cavity. The spectral position of the resonances depends on the geometrical structure of the μ-resonator and the effective refractive index of the system of the supported modes. Variations on the refractive index of the surrounding material will therefore shift the position of the resonances in a way that can be calibrated.

Even though the potential sensitivity would be larger for μ-rings, we have studied μ-disks structures, owing to the possibility of an electrical excitation without affecting the sensitive surface of the cavity.
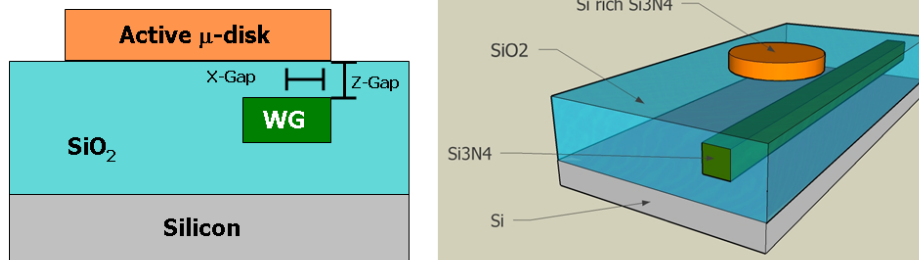


Figure 1. Left panel - Scheme of the cross section of the coupled, in which the variables Z-Gap and X-Gap are graphically defined. Right panel - 3D sketch representing the overall sensing device.

## 2.    DESIGN AND OPTICAL CHARACTERIZATION

### 2.1  Active material and Fabrication

Beyond the efficient room temperature visible PL, demonstrated for Si-nc embedded in Si nitride matrices by many groups [12], SRSN provides several appealing properties for fabricating compact and efficient emitting devices as its CMOS compatibility. It has already been demonstrated that by inducing the nucleation of Si clusters inside $Si_3N_4$, we obtain a compound having both good optical and electrical properties, represented by a bigger refractive index (n > 2 at 750 nm depending on the Si excess concentration), fast recombination rates [13] and efficient electrical injection. This last characteristic is due to the lower electron/hole injection barrier at the $Si$-$Si_3N_4$ interfaces [14] respect to others highly investigated materials, like the Si-rich silicon oxide (Si-SRSO). Furthermore the emission in the VIS region of the SRSN allows the use of Si-based detectors, which can be easily integrated with actual CMOS standard technology.

The realization of the coupled structure involved a three-step deposition process using two levels of photolithographic masks.  First of all a 150 nm thick $Si_3N_4$ passive layer was deposited on the $SiO_2$ layer (2 μm of thermally grown $SiO_2$ previously deposited on top of a crystalline Si wafer). Afterward a photolithographic process was executed in order to define the passive waveguides using a first mask level. Once defined such structures a further $SiO_2$ layer was grown, followed by a mechanical polishing process performed with the main goal of creating a planar $SiO_2$ top surface, acting as

layer separation between μ-disk and WG (represented in Figure 1 as the Z-Gap). The last deposition process was realized in order to grow the active SRSN layer: a 0.3 μm thick $Si_3N_4$ layer is deposited by the LPCVD technique, followed by a double Si ion implantation process at 90 and 150 keV in order to achieve a Si excess of 2.5%. At the end of the growth, the optically active circular structures (with radius between 3 and 10 μm) were defined by means of a second mask level.

## 2.2 Simulation

The main goal of the design process of the optical sensor is to find a mean point between the need of a high Q factor μ-resonators and intensity of the PL transmitted at the end of the bus WG. The Q factor is one of the prerequisites in order to obtain a good DL that we associate to the minimum refractive index change that provides a shifting equal to the FWHM of the resonance. Both parameters are indeed related to the vertical distance between the bottom of the disk and the top of the waveguide (*Z-gap*), which optimization is the real object of the design step. Contrarily to the passive coupled structures, where the critical coupling condition is almost mandatory for the waveguide-cavity relative position (it is indeed in this condition that the cavity is charged more efficiently through the waveguide), an optically active cavity the *Z-Gap* is a more relaxed parameter, since the light source is the resonator itself.

The optimization of the SRSN isolated active μ-disk and passive $Si_3N_4$ WG structures has been already described in [15], where high Q factors as high as $1.4x10^4$ and low losses WG under 1 dB/cm were demonstrated.

In order to evaluate the relative variation of Q and intensity inside the device, the whole structure has been reconstructed by FDTD simulation, [16] and two virtual intensity detectors have been placed in different positions of the system: one inside the disk on the opposite side respect to the WG position – used to evaluate the intensity of the resonances inside the μ-resonator – and the other at the end of the WG. This last detector helps us to obtain the value of the WGM intensity and Q after the coupling. We have to remark that the FDTD simulation package that we have exploited can take in account only the radiative losses of the structures and not the losses due to the material itself, that have been estimated in as high as 7dB/cm for the active material. [15]

Figure 4 shows the spectral behaviour of the Q factor, measured inside the disk for different *Z-Gap*: according to the previsions we can remark the decrease of Q value with the decreasing of the *Z-Gap*, which is inversely related to an increase of the overall cavity losses originated by the evanescent coupling with the waveguide. The more the WG is far from the μ-disk, the more the resonator behaves like an isolated cavity. It is afterwards clear that gap values below 0.2 μm (over-coupling distance) would not be of practical use, because the low Q will affect the DL of the structure. Further information comes out from the cross comparison between the intensity of the spectra obtained by the two detectors and the overall quality factors. By comparing the left and right panels of Figure 2 it is possible to understand that, while the WGM intensity within the disk increases with the vertical gap distance, the highest intensity values at the end of the WG are found at distances between 0.2 and 0.3 μm.
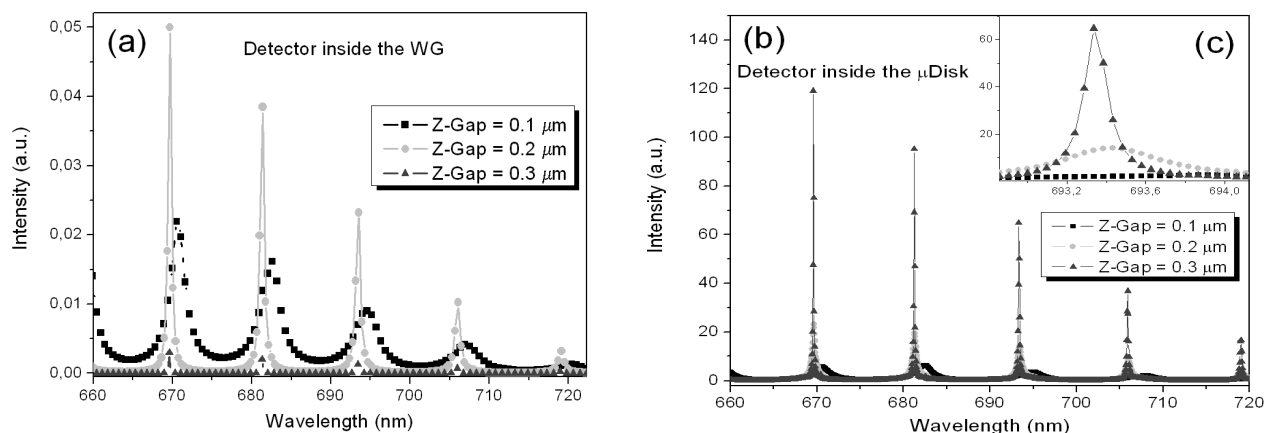


Figure 2. Left panel - Simulated WGM spectra of a 3 μm radius μ-disks, for different vertical gap values. The signal is provided by the detector placed on the waveguide. Right panel - Simulated WGM spectra measured inside the μ-resonator. The inset graphic shows a zoom of one particular resonance, putting in evidence the variation of Q factor in function of the gap distance

A gap value greater than 0.3 um will correspond to an under-coupling regime (overall Q above half of the Q of the isolated disk) while below 0.2 μm the regime is that of over-coupling and the presence of the waveguide starts to visibly modify even the real part of the effective refractive index, since the mode spectral position is shifted (Figure 4 (a)).

In summary, the intersection of the information obtained by the simulation suggested an optimum coupling distance between 0.2 and 0.3 μm. Therefore, taking into account this information, samples with different gaps within this range were realized (from 205 to 310 nm) by varying the oxide thickness between WG and μ-resonator.

FDTD simulations have also been performed on the coupled structure (having the same cross section described in Figure 1) in order to find the theoretical sensitivity of the device. In the proof of concept described in Section 3 we will use as analyte a Methanol-Ethanol solution having refractive indices of $n_{Met}$=1.318 and $n_{Et}$=1.3578 respectively: simulations have thus been performed by varying the third decimal figure of the refractive index of material surrounding the cavity, while monitoring the shifting in WGM resonant spectrum defined as $\Delta\lambda$.

With this information we can extract the correspondent Sensitivity of the device, defined as the fraction:

$$S = \frac{\Delta\lambda}{\Delta n} \qquad (1)$$

The *S* parameter represents the wavelength shift of a resonance ($\Delta\lambda$) as result of a change of one Refractive Index Unit (RIU) $\Delta n$. We have thus simulated the behaviour of a 7.5 μm radius disk coupled with a 1 μm wide WG with Z-Gap of 250 μm.

The obtained results are shown in Figure 3: in panel (a) is represented the spectral red-shift of one particular resonance as result of the same *n* values that we will use in the proof-concept measurements. The slope of the linear fit of the reported data, represented in the inset (b) bring to an *S* value of 60.82, comparable with that reported in the literature for other sensor measuring the refractive index variation. [16]
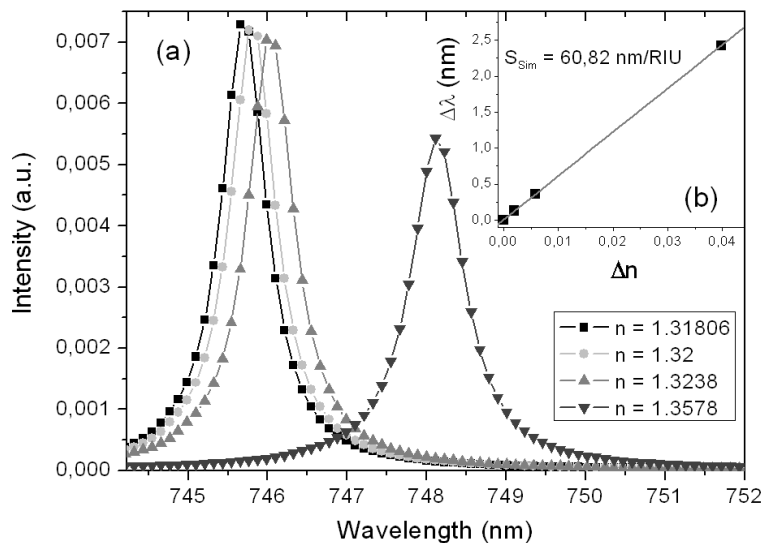


Figure 3. (a) Variation of the WGM position of a 7.5 μm radius disk due to a change of refractive index value. (b) linear slope of the maximum of one resonance reported in the Left panel, resulting in a Sensitivity of 60.82 nm/RIU

## 2.3 Optical characterization

The optical measurements presented in this manuscript were performed in a standard μ-PL setup, where the detection is performed on the plane of the μ-disks by means of a CCD camera placed behind a monochromator with focal length 750 mm and minimum resolution of 0.06 nm. A 370 nm solid state laser has been focused onto a single μ-disk by using a long working distance objective, allowing the formation of a circular pumping spot with minimum radius of

approximately 3 µm. The measurements of the coupled structures were made by pumping the µ-disks from the top and detecting the PL signal coming out from the passive waveguide.

The results of the optical characterization performed on the coupled device confirm the simulated qualitative behaviour as function of the increasing of the *Z-Gap*: to the lowering of the PL intensity measured at the output of the waveguide corresponds a rise of the *Q* factors of the resonances (represented in Figure 4 panel (a)).

Taking into account that the device with higher *Z-Gap* has the best result in terms of quality factor ($Q = 1.48 \times 10^3$) and since that the out coming intensity can be easily measurable by the CCD, we have decided to perform the sensoristic proof of concept principally on such devices with that *Z-Gap* value. The lowest Q respect to that reported in the case of the isolated structure [14] is due to a slight deformation of the cavity in correspondence of the coupling zone, due to a not perfect polishing process.

As we can see in panel (b) of Figure 4, reporting the both polarized spectra of a 7.5 µm radius disk surrounded by air and coupled with a 1 µm WG, in the described case only the TM polarization is coupled to the WG: this is probably because the *Z-Gap* is too high in order to extract a significant TE polarized signal (TM is less confined on the disk than TE, which improves the evanescent coupling efficiency).
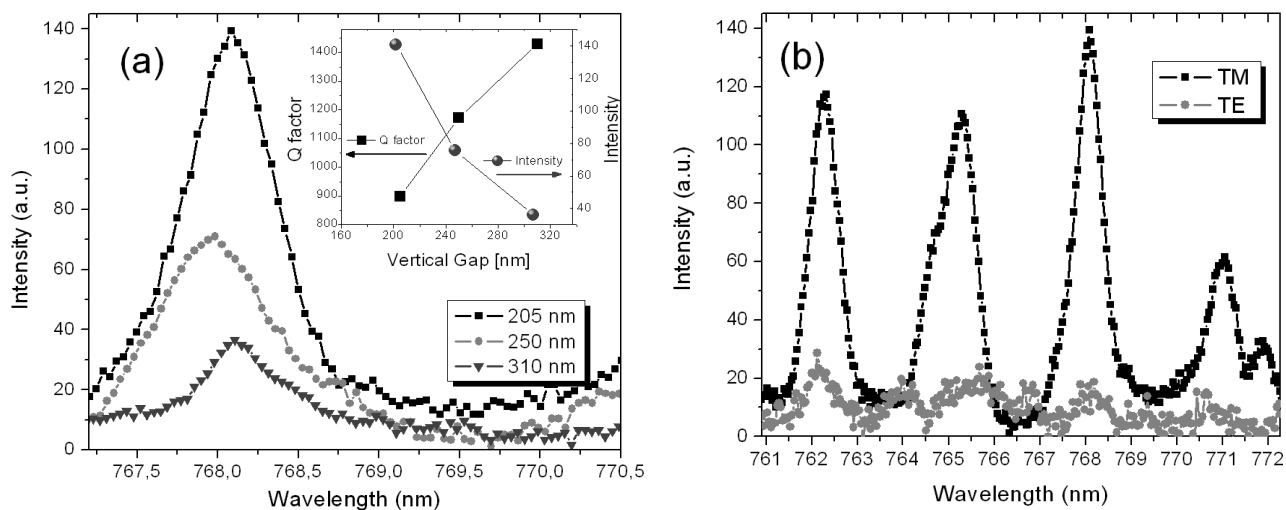


Figure 4. (a) - TM polarized µ-PL intensity of a resonance at about 768 nm for different gap distances between the bus waveguide and the µ-disk. In the inset the variation of intensity (gray spheres) and Q factor (black squares) are also plotted. (b) - TE (gray squares) and TM (black dots) polarized spectrum of a 10 µm µ-disk coupled with a 1 µm WG with ideal X-Gap of 0 µm and Z-Gap of 0.3 µm.

## 3.  SENSITIVITY AND DETECTION LIMIT

In order to evaluate the real sensitivity of the device, we have carried out µ-PL measurements by changing the environment of the µ-disks and following the spectral displacement of a certain resonance.  In particular we have varied the refractive index of the analyte as a function of the molar fractions of Methanol and Ethanol ($x_{Met}$ and $x_{Et}$ respectively) in a Methanol-Ethanol solution.

The molar refraction $R_M$ of a given substance can be expressed by the Lorentz-Lorenz equation:

$$R_M = \frac{n^2 - 1}{n^2 + 2} \cdot \frac{M}{\rho}$$

(2)

where $n$ is the refractive index of the solution at a certain wavelength, $M$ is the molecular mass and $\rho$ is the density. Those parameters take the following values for Methanol and Ethanol around $\lambda=750$ nm:

Table 1. Main parameters used in the preparation of the analytes

|  | **Methanol** | **Ethanol** |
|---|---|---|
| **R$_M$** | 7.36481158 | 12.81586633 |
| **n** | 1.31604 | 1.3578 |
| **M** | 32.04 | 46.07 |
| **r** | 0.7918 | 0.789 |

When dissolving the two substances, the molar refraction of the resulting solution is additive and becomes:

$$R_{M(Met,Et)} = x_{Met} \cdot R_{M(Met)} + x_{Et} \cdot R_{M(Et)} \tag{3}$$

According to the previous definitions, we have produced the following set of ten solutions with different molar fractions of the two substances:

Table 2. Molar fractions of the dissolutions of Methanol and Ethanol. In the third column is reported the resulting refractive index.

| x$_{Met}$ | x$_{Et}$ | n |
|---|---|---|
| 0.9658254 | 0.03417465 | 1.31806 |
| 0.9578315 | 0.0481685 | 1.31887 |
| 0.932111 | 0.67889 | 1.32 |
| 0.9030093 | 0.0969907 | 1.32159 |
| 0.8629 | 0.1371 | 1.3238 |
| 0.8033 | 0.1967 | 1.32691 |

This characterization has been performed on a coupled structure with $R = 7.5$ µm and *Z-gap* $= 310$ nm, which gave the best result in terms of Q. Finally, the proof of concept sensoristic measurement reported in the following section was made by pouring a drop of the analyte on the top of the disks by means of a µ-pipette.

The results of this measurement are showed in left panel of Figure 5, in which we can appreciate an overall resonance displacement of $\Delta\lambda= 0.5$ nm as a consequence of a change in refractive index of $\Delta n = 0.00885$ RIU

From the slope of the linear fit, realized taking in account all the points corresponding to the n values reported in Table 2 (dashed line in left panel of Figure 5) we can extract a maximum sensitivity of our device of 51.79 nm/RIU. According to the definition of DL related to the FWHM of the resonance [17] we have extracted a DL $= 1.2 \times 10^{-2}$.

The obtained values depend only on the material and the characteristics of the cavity and are only slightly lower than of some state-of-the-art ring resonator sensors. [9]
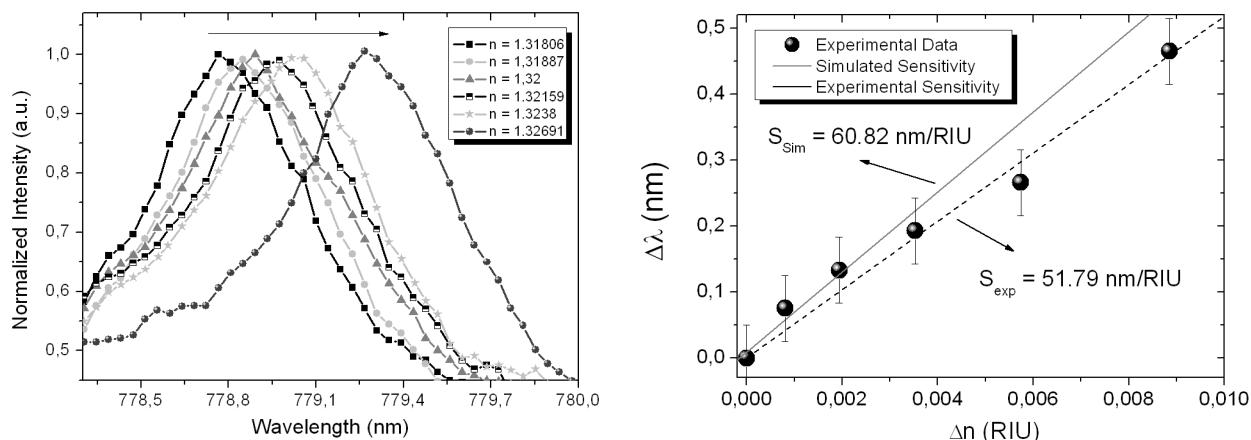
Figure 5. Left panel - Spectral displacement of a resonance obtained for the analytes with different n listed in Table 2. Right panel - Linear behavior of the $\Delta\lambda$ as a function of $\Delta n$, compared with the results of the simulation for the same structure. The slope of the linear fit is 51.79 nm/RIU.

It is worth to note that for analytes with higher Ethanol concentration (with molar fraction superior than $x_{Et}$=0.1967, not reported in Figure 5) the experimental data deviate from the theoretical prediction. This is probably a consequence of the fact that the characterisation associated to each analyte is done in sequence after the previous analyte evaporation and without cleaning the device between two consecutive measurements. We have proceeded in this way in order to preserve the alignment conditions. The Methanol used to make the solutions has a purity percentage of 99.9%, while the Ethanol presents a value of 99.8%, thus presenting a percentage of other volatile substances (e.g. Water, Acetone, Acetaldehyde or Isopropyl) and non volatile elements as metals. We believe that, due to the impurity percentage in high ethanol concentrations solutions, a deposition of a non volatile residual over the sample occurs, creating a thin layer over and aside the disk, slightly reducing the sensitivity of the system.

## 4. CONCLUSIONS

In this paper we have presented a thorough study on an optically active device composed by a high Q SRSN μ-disks vertically coupled to a passive low losses WG placed underneath.

The coupled structure has been previously simulated by FDTD package in order to find the best Z-Gap value in order to maximize the Q value while maintaining a useful value of intensity transmitted inside the WG. As further result of the simulation theoretical sensitivity of S=60.82nm/RIU has been calculated.

The optical characterization performed on the device demonstrated Q values up to $1.48 \times 10^3$ in the TM polarized spectrum, which are susceptible to be greatly improved through optimization of the fabrication process.

Through an experimental sensoristic proof of concept we have demonstrated that these structures are able to detect refractive index changes with sensitivities of 51.79 nm/RIU and minimum measured refractive index change of $1.2 \times 10^{-2}$.

On the basis of these results, and taking in account the high CMOS compatibility of the described device we believe that SRSN μ-disks have great potentiality to become building blocks of a photonic platform for sensing where demultiplexion and detection can be integrated on the same chip.

## REFERENCES

[1] X. Fan, I. M. White, S. I. Shopova, H. Zhu, J. D. Suter, Y. Sun, "Sensitive optical biosensors for unlabeled targets: A review", Analytica Chimica Acta, Vol. 680, pg. 8-26, (May 2008).

[2] C. Monat, P. Domachuk and B.J. Eggleton, "Integrated optofluidics: a new river of light", Nature Photonics, Vol 1, (February 2007).

[3] J.Dostalek, J. Homola, "Surface Plasmon resonance sensor based on an array of diffraction gratings for highly parallelized observation of biomolecular interactions", Sensors and Actuators B, Vol 129, pg. 303-307, (2008).

[4] B. J. Luff, J. S. Wilkinson, J.Piehler, U. Hollenbach, J. Ingenhoff and N. Fabricius, "Integrated Optical Mach-Zehnder Biosensor", Journal of Lightwave Technology, Vol. 16, No.4, pg. 583, (April 1998).

[5] R. G. Heideman and P. V. Lambeck, "Remote opto-chemical sensing with extreme sensitivity: design, fabrication and performance of a pigtailed integrated optical phase-modulated Mach-Zehnder interferometer system", Sen. Actuators B, 61, pg 100-127, (1999).

[6] B. J. Luff, R. D. Harris, J. S. Wilkinson, R. Wilson and D. J. Schiffrin, "Integrated optical directional coupler biosensor," Optics Letter., Vol. 21, pg. 618–620, (1996).

[7] L. Jiang and S. Pau, "Integrated waveguide with a microfluidic channel in spiral geometry for spectroscopic applications", App. Phys. Lett. 90, 111108, (March 2007).

[8] M.G. Scullion, A. Di Falco, T.F. Krauss, "Slotted photonic crystal cavities with integrated microfluidics for biosensing applications", Biosensors and Bioelectronics", Vol 27, Issue 1, p. 101-105, 15 September 2011.

[9] A. Yalçin, K.C. Popat, J.C. Aldridge, T.A. Desai, J. Hryniewicz, N. Chbouki, B.E. Little, O. King, V.Van, S. Chu, D. Gill, M. Anthens-Washburn, M.S. Unlu, B.B. Goldberg, "Optical sensing of biomolecules using microring resonators", IEEE J. Sel. Top. Quantum Electron., Vol 12, No. 1, (January 2006).

[10] K. De Vos, I. Bortolozzi, E. Schacht, P. Bienstman, R. Beats, "Silicon-on-insulator microring resonator for sensitive label-free biosensing", Optics Express, Vol 15, No. 12, (June 11, 2007).

[11] R.W. Boyd, and J. E. Heebner, "Sensitive disk resonator photonic biosensor", Applied Optics, Vol. 40, No. 31, (November, 2001).

[12] N.M. Park, C.J.Choi, T.Y. Seong, S.j.Park, "Quantum Confinement in Amorphous Silicon Quantum Dots Embedded in Silicon Nitride" Phys. Rev. Lett. 86, 1355, 2001.

[13] L.Dal Negro, J. H. Yi, J. Michel, L. C. Kimerling, T.-W. F. Chang, V. Sukhovatkin, and E. H. Sargent, "Light emission efficiency and dynamics in silicon-rich silicon nitride films", Applied Physics Letters, No. 88, 233109, (2006).

[14] Y. Berencén, J. Carreras, O. Jambois, J. M. Ramírez, J. A. Rodríguez, C. Domínguez, C. E. Hunt, and B. Garrido, "Metal-nitride-oxide-semiconductor light-emitting devices for general lighting", Optics Express, Vol.19, Issue S3, pg. A234-244, (2011).

[15] F. Ferrarese Lupi, , D. Navarro-Urrios, J. Monserrat, C. Dominguez, P. Pellegrino, and B. Garrido, "High Q light-emitting Si-rich $Si_3N_4$ microdisks", Optics Letters, Vol. 36, No. 8, (April 15, 2011).

[16] A.F. Oskooi, David Roundy, M. Ibanescu, P. Bermel, J. D. Joannopoulos, S.G. Johnson, "MEEP: A flexible free-software package for electromagnetic simulations by the FDTD method", Computer Physics Communications, Vol. 181, pg. 687-702, (January 8, 2010).

[17] F. Ferrarese Lupi, , D. Navarro-Urrios, J. Rubio-Garcia, J. Monserrat, C. Dominguez, P. Pellegrino, and B. Garrido, "Visible Light emitting Si-Rich $Si_3N_4$ µ-disk resonators for sensoristic applications", J. Ligth. Tech., Vol. 30, No. 1, pg. 169-174, (January 1 2012).